JOURNAL OF PROPULSION AND POWER
Vol. 19, No. 3, May–June 2003

Model of an Electrothermal Pulsed Plasma Thruster

Michael Keidar* and Iain D. Boyd†
University of Michigan, Ann Arbor, Michigan 48109
and
Isak I. Beilis‡
Tel Aviv University, 69978 Tel Aviv, Israel

The physical processes of a pulsed discharge in a dielectric (Teflon®) cavity of a coaxial electrothermal pulsed plasma thruster (PPT) are analyzed. The considered PPT has this central Teflon cavity to produce a high-pressure cloud of ablation products during the discharge pulse. The mathematical model includes the Teflon thermal conduction, the plasma energy balance, the mass and momentum conservation in a quasi-neutral plasma region, and the relation between the plasma parameters in a nonequilibrium layer near the ablated Teflon surface. It is found that the plasma parameter variation along the cavity length is an important feature of the ablation-controlled discharge in the cavity that affects the plasma energy balance, mass and momentum conservation, and thermal conductivity. Performance characteristics of the PPT such as mass ablation and impulse thrust bit are calculated. Predicted plasma temperature, ablation rate, and gasdynamic thrust are found to be in agreement with experimental data.

Nomenclature

A	=	cavity cross section
a	=	thermal diffusivity
C_p	=	specific heat
I_{bit}	=	impulse bit
j	=	current density
j_{eth}	=	random electron current density
j_i	=	ion current density
L	=	cavity length
m	=	heavy particle mass
n_e	=	plasma density
n_s	=	density at the surface
n_1, n_2	=	densities
P	=	pressure in the cavity
P_{eq}	=	equilibrium pressure
R_a	=	cavity radius
T_p	=	plasma temperature
T_1, T_2	=	temperatures
T_s	=	Teflon® surface temperature
Q_F	=	heat due to the particle convection
Q_j	=	joule heat
Q_r	=	radiation heat
V	=	plasma velocity
V_1	=	velocity at the Knudsen layer edge
Z_i	=	ion charge number
Γ	=	ablation rate, kg/m^{2}s
ΔH	=	ablation heat
λ	=	thermal conductivity
ρ	=	mass plasma density
σ	=	plasma conductivity

Received 27 July 2001; revision received 1 August 2002; accepted for publication 7 December 2002.

*Research Scientist, Department of Aerospace Engineering. Member AIAA.
†Professor, Department of Aerospace Engineering. Senior Member AIAA.
‡Professor, Electrical Discharge and Plasma Laboratory, Department of Interdisciplinary Studies, Fleischman Faculty of Engineering, P.O. Box 39040.

I. Introduction

PULSED plasma thrusters (PPTs) have the combined advantages of system simplicity, high reliability, low average electric power requirement, and high specific impulse.[1] The PPT is considered as an attractive propulsion option for orbit insertion, drag makeup, and attitude control of small satellites. PPTs, however, have very poor performance characteristics, with an efficiency[2] of about 10%, leaving an opportunity for substantial improvement. To improve the PPT performance, several directions are being considered, such as elimination of late-time ablation, choice of the proper current waveform, etc.[3]

Currently new PPT devices with electromagnetic[4,5] and electrothermal mechanisms are under development[6–8] that reflect the increased interest in these types of thrusters. Recently electromagnetic PPT was successfully operated for pitch axis control on the EO-1 spacecraft.[9,10] In this study we concentrate on PPT devices developed at the University of Illinois, the PPT-4 and PPT-7 (Refs. 6, 7, and 11). This is an electrothermal device that derives most of its acceleration from the electrothermal or gasdynamic mechanism. As schematically shown in Fig. 1, this thruster is axially symmetric, and a discharge occurs between the annular cathode at the thruster exit plane and the circular metal anode located at the far end of a cylindrical cavity made of Teflon®. The plasma generated inside this cavity is accelerated in a diverging dielectric nozzle that is attached to the downstream end of the cavity. The device has a pulse length of about 10 μs, and the overall specific impulse was measured to be 850 s.

The main physical processes in this type of PPT occur in the Teflon cavity in a similar way to an ablation-controlled discharge. Rapid heating of a thin dielectric surface layer leads to decomposition of the material of the wall. As a result of heating, decomposition, and partial ionization of the decomposition products, the total number of particles increases in the cavity. The problem of the ablation-controlled discharge also has a more general interest because it can be used for various applications such as electric fuses, circuit breakers, soft x ray, and extreme ultraviolet sources.[12–15] In these devices, the discharge energy is principally dissipated by ablation of wall material, which then forms the main component of the discharge plasma. Therefore, these type of discharges have a lot similarities with electrothermal PPT considered in this paper.

An important concern of the successful operation of a PPT on a spacecraft is a complete assessment of the spacecraft integration effects. The Teflon-fed PPT plume contains various ion and neutral species of carbon and fluorine due to propellant decomposition and

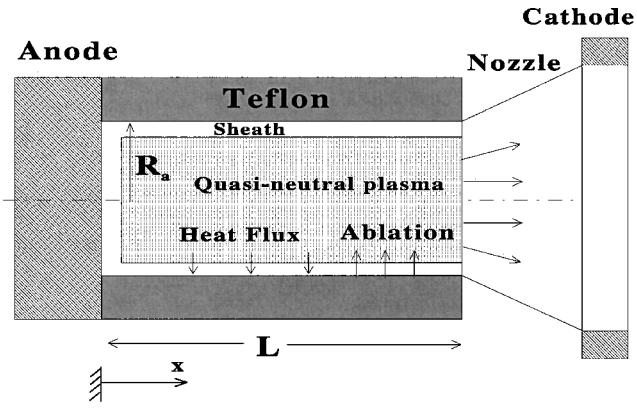

Fig. 1a Schematic of the problem geometry (not to scale).

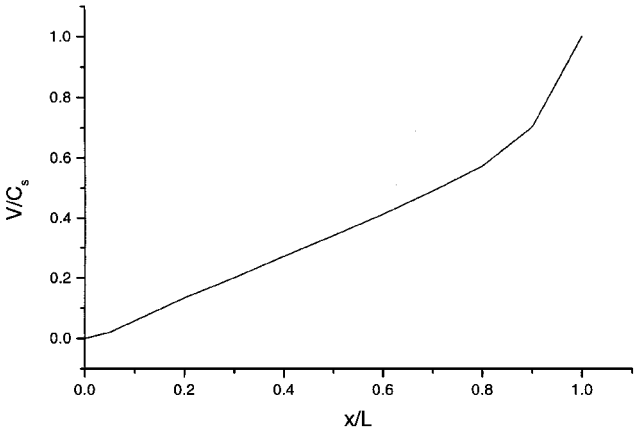

Fig. 1b Plasma velocity distribution along the cavity length.

possible electrode erosion. Therefore, the main integration issue is the deposition of highly condensable PPT plumes on spacecraft surfaces. To predict the spacecraft integration effect, an exhaust plume simulation is required. Some attempts at PPT plume simulation using hybrid direct simulation Monte Carlo (DSMC) and particle-in-cell (PIC) simulations were performed recently.[16,17] In Ref. 16, however, some artificial starting conditions were employed. Accurate plume modeling requires the accurate formulation of boundary and initial conditions that in turn rely on the device model. This was attempted in Ref. 18, where a model of the Teflon ablation and plasma discharge processes is described. The model was calibrated against mass ablation data for the PPT-4. Then, in Ref. 17, the time-dependent plasma density, velocity, and temperature distributions at the thruster nozzle exit obtained in Ref. 18 were used as boundary conditions to perform a particle-based PIC–DSMC computation of the electrothermal PPT plume. From direct comparison with experimental data, it was concluded that the main plasma plume features were captured, although the simulation underestimated the plasma densities at later times in the discharge. The underprediction of the plasma density is a result of the basic assumption of the plasma-generation model in considering the plasma to be uniform in the cavity.[18] Further understanding of the physical processes involved requires more detailed analyses including the spatial variation of plasma parameter distributions along the cavity and a more sophisticated ablation model. These are the primary objectives of the present paper.

II. Ablation-Controlled Discharge Model

We consider the plasma generation processes (ablation, heating, radiation, ionization, etc.) and plasma acceleration along a Teflon cavity of a pulsed electrical discharge. Figure 1 shows some characteristic regions such as the Teflon bulk, the electrical sheath near the dielectric, and the quasi-neutral plasma. Different kinetic and hydrodynamic phenomena determine the main features of the plasma flow including plasma joule heating, heat transfer to the dielectric, and electrothermal acceleration of the plasma up to the sound speed at the cavity exit. We discuss the model in different regions and the full system of equations including the final expressions obtained in Ref. 18.

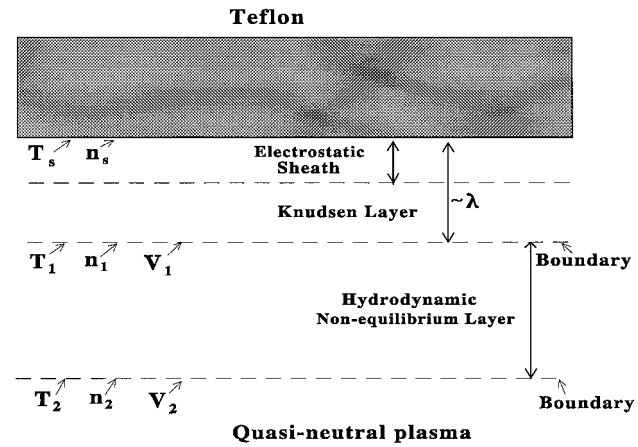

Fig. 2 Schematic presentation of the layer structure near the ablated surface.

A. Sheath

It was concluded previously[18] that during the discharge pulse, a quasi-steady sheath structure is formed and that under typical PPT conditions this sheath is unmagnetized in the self-magnetic field generated during the pulse. The potential drop of the electrostatic sheath near the Teflon wall, shown schematically in Fig. 2, is negative to repel the excess thermal electrons. Under these conditions, the potential drop in the sheath can be calculated as

$$U_d = -T_p \ln(j_{\text{eth}}/j_i) \tag{1}$$

where j_i is the ion current given by the expression

$$j_i = 0.4 e Z_i n_e (kT_p/m)^{\frac{1}{2}}$$

B. Teflon Ablation

The Teflon ablation is modeled in the framework of the approximation[19] based on a previously developed kinetic model of metal evaporation into a surrounding plasma.[20] To understand the mathematical description of the model used, we distinguish two different layers between the surface and the plasma bulk (Fig. 2): 1) a kinetic nonequilibrium Knudsen layer adjusted to the surface with a thickness of about one mean free path and 2) a collision-dominated hydrodynamic layer with thermal and ionization nonequilibrium. The plasma–wall transition layer includes also an electrical sheath described in the preceding section. This model makes it possible to calculate the plasma parameters (density and temperature) at the interface between the kinetic and hydrodynamic layers (boundary 1 in Fig. 2) if the velocity at this boundary V_1 is known. The velocity V_1 can be determined by coupling the solution of the hydrodynamic layer and the quasi-neutral plasma. For known velocity and density at this interface, it is possible to calculate the ablation rate. In the hydrodynamic layer, the relation between the velocities, temperatures, and densities at the boundaries 1 and 2, as well as the ablation rate, are formulated according to Ref. 19 in the form

$$\Gamma = m V_1 n_1 = n_1 \left[(2kT_1/m) \cdot (T_2 n_2 / 2T_1 - n_1/2) \Big/ \left(n_1 - n_1^2/n_2 \right) \right]^{0.5} \tag{2}$$

The average atomic mass for two species (carbon and fluorine) was assumed to be equal $m = 17$, which takes into account nuclei fractions ratio. Expression (2) was derived by coupling mass and momentum equations in the hydrodynamic layer. The system of equations is closed if the equilibrium vapor pressure can be specified that

determines parameters n_s and T_s at the Teflon surface. In the case of Teflon, the equilibrium pressure formula is used[1,3,21]:

$$P_{\text{eq}} = P_c \exp(-T_c/T_s) = n_s k T_s \tag{3}$$

where $P_c = 1.84 \times 10^{15}$ N/m^2 and $T_c = 20{,}815$ K are the characteristic pressure and temperature, respectively. As will be shown in the "Results" section, the radial velocity V_1 that determines the evaporation rate is small in comparison with the sound speed. This result is a reflection of the fact that the Teflon ablation under typical electrothermal PPT conditions is strongly affected by the presence of the plasma. In the free evaporation case, the velocity V_1 should be equal to the local sound speed.[22]

C. Quasi-Neutral Plasma Analyses

The energy transfer from the plasma column to the wall of the Teflon cavity consists of the heat transfer by particle fluxes and radiation heat transfer. Previous models of the ablation-controlled discharge show that the axial pressure and velocity variations are much greater than those in the radial direction.[23,24] Therefore, we will assume that all parameters vary in the axial direction x (Fig. 1), but are uniform in the radial direction. Plasma parameters also have rapid temporal variation during the discharge pulse, so that there is a concern about the possibility of establishing local thermodynamic equilibrium (LTE). For instance, in a homogeneous transient plasma,[25] complete LTE may be obtained in 0.3 μs for a helium plasma with electron density of 10^{24} m^{-3}. An estimation of the characteristic times for ionization and recombination has shown that the ionization and recombination timescales for ground states of C and F are less than the typical time for discharge parameter changes.[26] Therefore, LTE establishing may be considered during the discharge pulse, which is about a few microseconds. An estimate of the relaxation time for elastic collisions has shown that, in a plasma with density of 10^{22}–10^{24} m^{-3} and an electron temperature of 1–3 eV, equilibrium of electrons, ions, and neutrals is established on a timescale less then a microsecond (Ref. 27). Thus, the present model considers temperature equilibrium $T_e = T_i = T_p$, where T_p is the plasma temperature.

Starting from the preceding considerations, we developed a simplified model of the discharge in the dielectric cavity using the following basic assumptions: 1) the plasma is quasi neutral and 2) the plasma column is in LTE.

The axial component of the mass and momentum conservation equations reads

$$A\left(\frac{\partial \rho}{\partial t} + \frac{\partial(\rho V)}{\partial x}\right) = 2\pi R_a \Gamma(t, x) \tag{4}$$

$$\rho\left(\frac{\partial V}{\partial t} + \frac{V \partial V}{\partial x}\right) = -\frac{\partial P}{\partial x} \tag{5}$$

The energy balance equation can be written in the form[18]

$$\frac{3}{2} n_e \left(\frac{\partial T_p}{\partial t} + \frac{V \partial T_p}{\partial x}\right) = Q_J - Q_r - Q_F, \qquad Q_J = \frac{j^2}{\sigma}$$

$$Q_r = A Z_i^2 n_e^2 T^{\frac{1}{2}} (1 + \chi_g), \qquad Q_F = \frac{2 j_i}{R_a}(2T + U_d + T) \tag{6}$$

According to Zemskov et al.,[26] the radiation in continuum from a C + 2F plasma in the considered parameter range provides the main contribution. The radiation energy flux Q_r includes the radiation for a continuum spectrum based on a theoretical model.[28] In the expression for Q_r the coefficient A is the constant (1.6×10^{-38} in SI units) and $\chi_g = E_g/T_p$, with E_g as the energy of the low excited state. The particle convection flux Q_F includes energy associated with electron and ion fluxes to the dielectric wall that leads to plasma cooling. It was shown previously that the energy is carried off mainly by the particle convection.[18] Our estimations and previous calculation show[18] that the electron temperature varies only slightly with axial position, and therefore, we performed the calculation assuming $\partial T_p/\partial x = 0$.

Radiation and convection heat fluxes from the plasma to the cavity wall (Fig. 1) determine the thermal regime of the Teflon. The temperature inside the Teflon wall can be calculated from the heat transfer equation:

$$\frac{\partial T}{\partial t} = \frac{a \partial^2 T}{\partial r^2} \tag{7}$$

This is the one-dimensional equation in the radial direction. This assumption can be made because the heat-layer thickness near the surface is smaller than the Teflon cylinder curvature R_a and also less than the characteristic length of plasma parameter changes in the axial direction. To solve this equation, boundary and initial conditions must be specified[18]:

$$-\frac{\lambda \partial T}{\partial r}(r = 0) = q(t) - \Delta H \cdot \Gamma - C_p(T_s - T_0)\Gamma$$

$$\frac{\lambda \partial T}{\partial r}(r = \infty) = 0, \qquad T(t = 0) = T_0 \tag{8}$$

where $r = 0$ corresponds to the inner dielectric surface, which is in contact with a plasma, ΔH is the ablation heat, Γ is the rate of Teflon ablation per unit area, T_0 is the initial temperature, and $q(t)$ is the heat flux, consisting of the radiative and particle convection fluxes, and T_s is the Teflon surface temperature. The solution of this equation is considered for two limiting cases of substantial and small ablation rate very similar to that described in Ref. 18. Note that the thruster operates with a typical pulse rate of about 1 Hz in laboratory conditions. Thus, it is possible that the Teflon surface temperature during the time between pulses may be higher than room temperature, which may increase the total mass ablation. However, calculation of the late time ablation shows that it consumes no more that 1 μg per pulse.[18]

Having calculated the plasma density and plasma temperature [Eqs. (1–3)], one can calculate the chemical plasma composition considering LTE in the way described previously.[18,29,30] According to calculations,[29,30] in the considered range of electron temperature (1–3 eV) and plasma density (10^{21}–10^{24} m^{-3}), the polyatomic molecules C_2F_4 almost fully dissociate. Therefore, we will start our consideration from the point when we have gas containing C and F. The Saha equations for each species (C and F) are supplemented by the conservation of nuclei and quasi neutrality. The complete system of equation for chemical composition is presented in Ref. 18.

III. Results

In this section, we present results of the calculation of the temporary and spatial variation of the plasma parameters in the Teflon cavity. As a working example, one configuration of an electrothermal PPT is considered: PPT-4 (Refs. 6 and 11). Most of the results are presented for PPT-4 with the following baseline geometry and discharge parameters: anode radius $R_a = 3.05$ mm and cavity length $L = 8.3$ mm, and pulse duration of about 10 μs (Refs. 6 and 11). The current pulse has a peak of about 8 kA and is nonreversing because of the use of a diode across the capacitor. (It is shown subsequently for reference.) The current reaches a peak at about 3 μs.

The boundary condition used for Eqs. (4) and (5) at $x = 0$ is $\partial n/\partial x = 0$. The plasma accelerates in the axial direction due to the pressure gradient and achieves the sound speed at the cavity exit plane, $x = L$ (Fig. 1). The plasma velocity distribution is shown in Fig. 1b. One can see that the plasma is significantly accelerated near the cavity exit. Burton et al. obtained similar flowfield development in a liquid-injected capillary discharge,[31] when the plasma flow approaches steady-state conditions.

A. Plasma Parameters

The temporal and axial distribution of the radial velocity at the external boundary of the kinetic layer V_1 (boundary 1, Fig. 2) is shown in Fig. 3. In the entire region, the normalized velocity remains smaller than 1. This reflects that the Teflon vapor velocity is subsonic due to the presence of the discharge plasma and freestream flow condition at the cavity exit.

The time evolution of the plasma temperature T_p is shown in Fig. 4. It can be seen that the electron temperature initially increases rapidly and peaks at about 3.5 eV and then decreases to 1 eV toward the pulse end. For comparison, we also plotted experimental results[6,11] measured in the plume. In the experiment, the peak electron temperature was measured to be in the range of 2–2.6 eV and decreases down to about 1 eV and varies slightly with axial distance from the thruster exit plane. The experimental data presented here were taken at several probe locations at 10–18 cm from the thruster exit plane, and therefore one can expect a shift of timescale. This shift (approximately 7 μs) is equal approximately to the plasma flight time from the cavity to the plane where data were taken according to our simulations.[17] One can see that the model predictions and experimental data have a similar trend, which indicates that the model prediction agrees reasonably with the experimental data. For reference we show also experimental current waveform[6,11] in Fig. 4.

The pressure distribution in the cavity is shown in Fig. 5. During the pulse plasma, pressure peaks at about 20 atm. The ablation rate calculated using Eq. (2) and impulse bit are shown in Fig. 6. One can see that the ablation rate peaks at about 120 kg/m^{2}s at 2.5 μs and then rapidly decreases. The peak of the ablation rate approximately corresponds to the current peak (Fig. 4). Note that in the experiment the average ablation rate was estimated to be about 30 kg/m^{2}s (Refs. 6 and 11). The comparison of the predicted and measured total ablation rates is presented later.

The temporal variation of the Teflon surface temperature at several locations along the cavity is shown in Fig. 7. The temperature

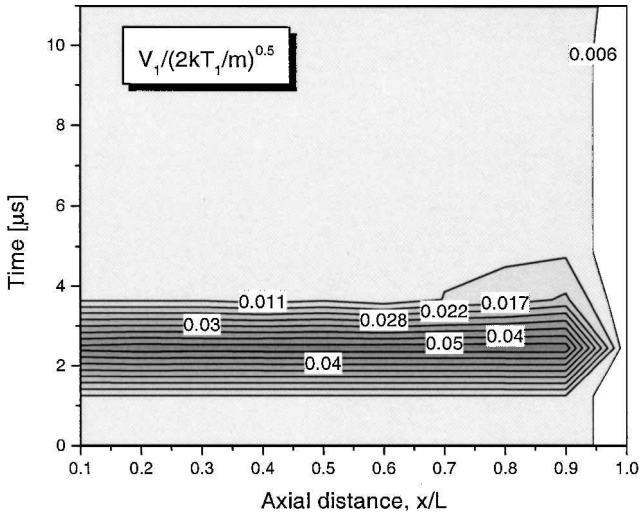

Fig. 3 Velocity at the outer boundary of the Knudsen layer V_1 as a function of axial distance and time.

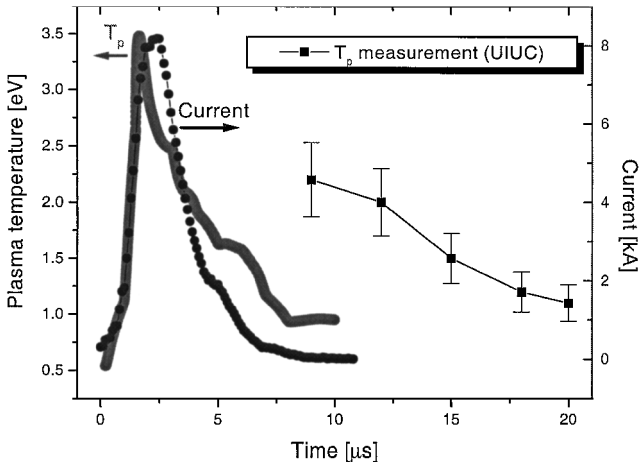

Fig. 4 Temporal variation of the electron temperature in the cavity, experimental data taken from Ref. 6 and experimental current waveform taken from Refs. 6 and 11.

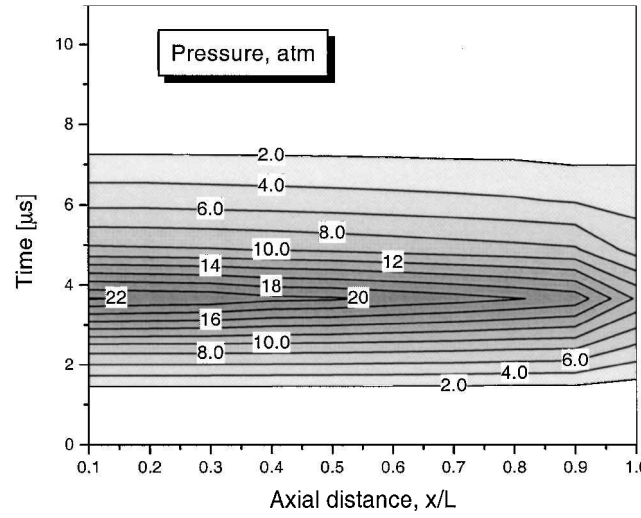

Fig. 5 Temporal and axial variation of total pressure.

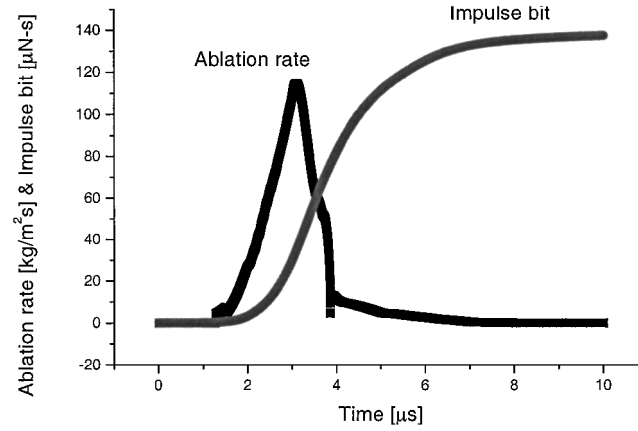

Fig. 6 Ablation rate and impulse bit vs time.

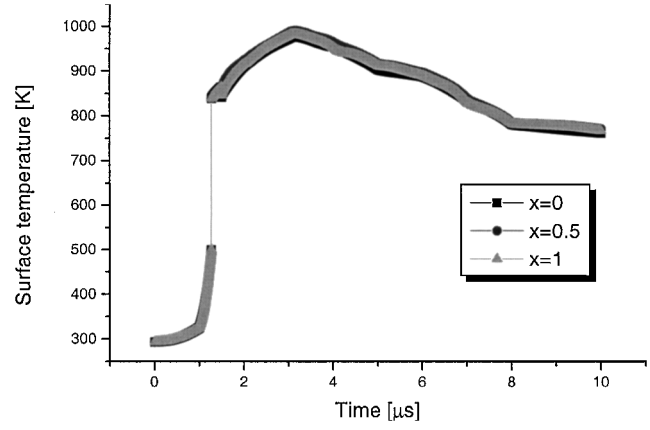

Fig. 7 Temporal variation of the Teflon surface temperature with position along the cavity as a parameter.

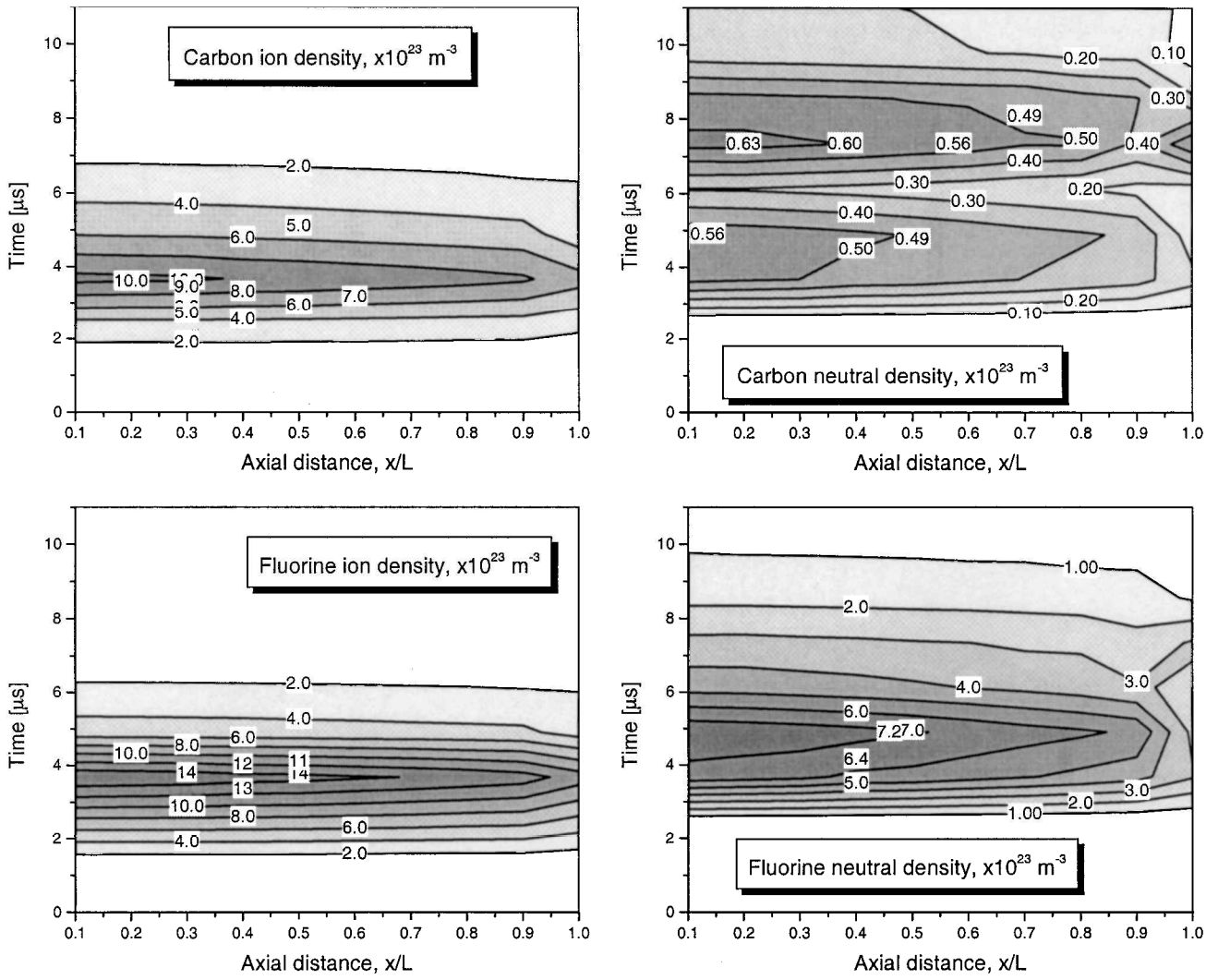

Fig. 8 Temporal and spatial variation of the chemical species during discharge pulse.

sharply increases during the first 4 μs of the discharge pulse and peaks at about 1000 K. One can see that the temperature varies only slightly along the cavity, so that the assumption of Teflon surface temperature uniformity introduced previously[18] may be considered as reasonable.

Figure 8 shows the temporal and spatial variation of the different ion and neutral species. Both ion species densities peak at early times (about 3 μs), whereas neutral species peak later. The relative concentration of the species changes along the cavity length and also during the discharge pulse. One can see from Fig. 8 that the model predicts that initially plasma in the cavity is strongly ionized, whereas after about 3 μs, the ionization degree decays.

B. Thruster Performance

The calculated Teflon mass ablated per pulse is shown in Fig. 9 as a function of cavity length and radius. Generally, the ablated mass increases with increasing cavity length and decreasing cavity radius. The ablated mass increases with the cavity length due to increasing the surface area exposed to the plasma heating. However, when the cavity radius increases, the ablated mass decreases, although the ablated surface area increases. This effect is a result of the decreases in the power density (Joule heat) as the cavity radius increases. From comparison with experiment, it can be shown that the model underpredicts the ablation mass by about 25%. However, note that some mass can be ablated in the form of large particulates. This effect for one particular PPT was estimated to be up to 40% of the total ablated mass,[32] which could account for the underpredictionof the model. The ablation in the particulate phase was not considered in the present paper.

To assess the ability of the model to predict some thruster performance characteristics, we calculated the thrust impulse bit as a function of cavity geometry and compared with experimental data. The gasdynamic thrust impulse is generated due to the pressure force on the anode. The total impulse generated during the pulse is calculated as

$$I_{\text{bit}} = \pi R_a^2 \int P \, \mathrm{d}t$$

where $P = kT_p(n_a + n_i + n_e)$ is the pressure in the cavity, n_a is the neutral atom density, n_i is the ion density, and n_e is the electron density. We integrate the pressure during the discharge to calculate the thrust impulse bit produced in the Teflon cavity. However, the PPT-4 thruster also has a nozzle with an area ratio of about 100. Such a nozzle may increase the thrust up to a factor of $\beta = 1.7$ (Ref. 33). The plasma flow in the nozzle is not considered in the present paper, and therefore, we will use the nozzle factor as a parameter. The thrust impulse bit dependence on the cavity length is shown in Fig. 10. One can see that the impulse bit increases by a factor of three when L increases from 3 up to 25 mm similar to that obtained in the experiment.[6,11] Note that, in the entire range of L, the best agreement between the model and experiment is obtained for $\beta = 1.5$. This means that the nozzle has an important effect according to the model.

IV. Discussion

The calculations show that there is a strong correlation between the peaks of all parameters (plasma density and temperature, Teflon surface temperature, and ablation rate) and the peak of the discharge

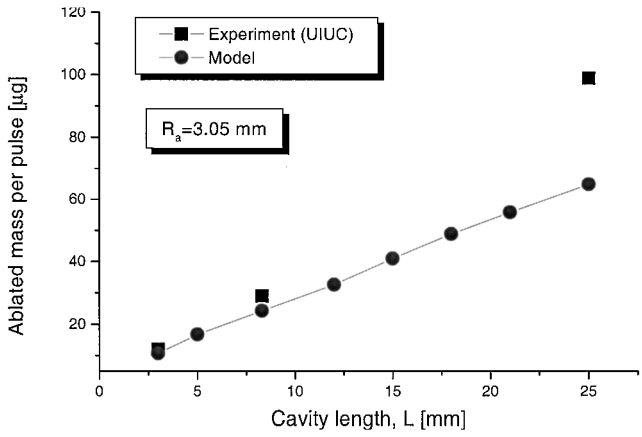

a)

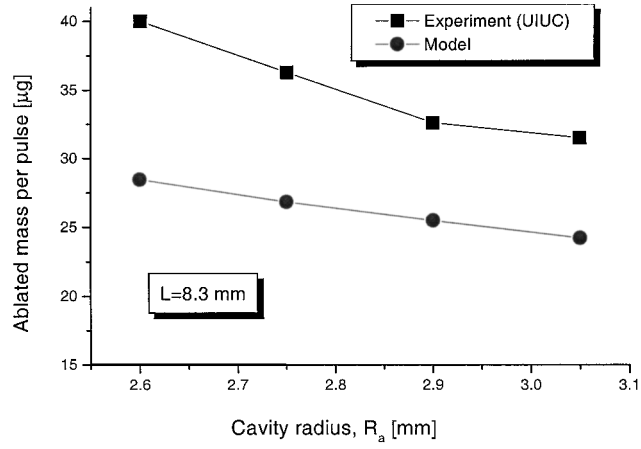

b)

Fig. 9 Ablated mass as a function of cavity geometry and comparison with experiment[6,11]: a) constant cavity radius and b) constant cavity length.

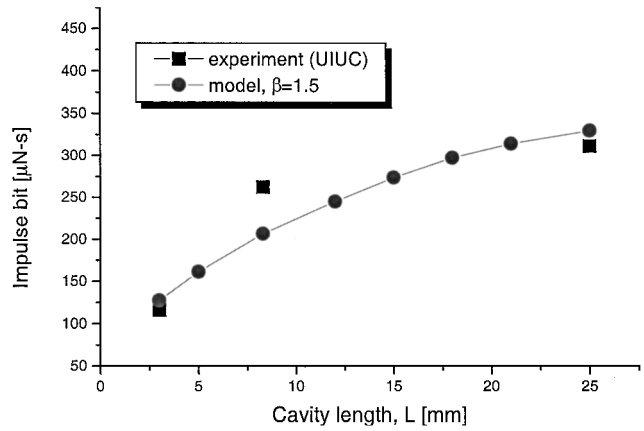

Fig. 10 Thrust impulse bit variation with cavity length with nozzle factor β as a parameter and comparison with experiment; experimental data taken from Refs. 6 and 11.

current. This is an expected result because the LTE assumption is employed in the model and because the discharge current affects the main energy input, Joule heat.[18] However, this is an important result because it shows that a way to control the temporal variation of plasma parameters and ablation rate in the this type of PPT is by changing the current waveform.

The axial plasma density variation affects the heat flux to the surface and, therefore, the thermal regime of the Teflon. Whereas the plasma density varies by a factor of two, the spatial variation of the Teflon surface temperature is small, as shown in Fig. 7. In addition, the spatial variation of the plasma density also affects the Teflon ablation because in our model the ablation is coupled with the bulk plasma. Therefore, spatial variation of the ablation rate (velocity V_1 that determines the ablation rate) shown in Fig. 3 becomes more important near the cavity exit, where the density variation is large (Fig. 8).

The more sophisticated ablation model takes into account the returned atom flux that forms in the nonequilibrium Knudsen layer during the ablation. This approach makes possible the calculation of the ablation rate when the propellant surface temperature, density, and temperature in the plasma bulk region are known. In this sense, the present model is different from previously used approaches (Refs. 17 and 18 and references therein), where the ablation rate was determined by the surface temperature only. It was demonstrated that this ablation model could be coupled with a plasma discharge model and predict ablation mass in good agreement with the experimental data without using a free fitting parameter.

The energy balance shows similar results to the previous study[18] that the input energy (from the Joule heat) is mainly carried off by particle convection and radiation, when radiation consumes about 10% of the energy output. However, an important issue, which is related to the ablation discharge model, is a plasma radiation approach. In the present paper, similar to the previous model,[18] it was assumed that the main radiation energy losses are due to the radiation in a continuum spectrum.[34] This assumption can be justified by that, during the discharge pulse, the plasma density lies in the range of 10^{23}–10^{24} m^{-3} and can be considered high enough for the continuum spectrum approach.[35]

V. Conclusions

A self-consistent analyses of the electrical discharge in the Teflon cavity of coaxial electrothermal PPTs shows that there is a coupling between the bulk plasma parameters and Teflon ablation. This happens because the ablation model takes into account the returned atom flux that formed in the nonequilibrium Knudsen layer during the ablation. As a result, the velocity at the kinetic layer edge (which determines the ablation rate) is much smaller than the sound speed. During the discharge pulse, the plasma density peaks at about 10^{24} m^{-3}, electron temperature peaks at about 3.5 eV, and the ablation rate peaks at about 120 kg/m^2s, which is in the good agreement with simplified model predictions published earlier.[18] Electron temperature and performance characteristics of the PPT such as mass ablation and impulse thrust bit were calculated and compared with available experimental data. Good qualitative and quantitative agreement was obtained.

Acknowledgments

The authors gratefully acknowledge the financial support by the Air Force Office of Scientific Research through Grant F49620-99-1-0040. We also acknowledge R. L. Burton from the University of Illinois, Urbana–Champaign, for valuable discussions.

References

[1]Burton, R. L., and Turchi, P., "Pulsed Plasma Thruster," *Journal of Propulsion and Power*, Vol. 14, No. 5, 1998, pp. 716–735.

[2]Vondra, R. J., "The MIT Lincoln Laboratory Pulsed Plasma Thruster," AIAA Paper 76-998, 1976.

[3]Turchi, P. J., "Directions for Improving PPT Performance," *Proceeding of the 25th International Electric Propulsion Conference*, (The Electric Rocket Propulsion Society, Worthington, OH, 1997) Vol. 1, 1998, pp. 251–258.

[4]Antonsen, E., Burton, R. L., and Rysanek, F., "Energy Measurements in a Coaxial Electromagnetic Pulsed Plasma Thruster," AIAA Paper 1999-2292, July 1999.

[5]Gulczinski, F., III, Dulligan, M., Lakes, J., and Spanjers, G., "Micropropulsion Research at AFRL," AIAA Paper 2000-3255, July 2000.

[6]Bushman, S. S., and Burton, R. L., "Heating and Plasma Properties in a Coaxial Gasdynamic Pulsed Plasma Thruster," *Journal of Propulsion and Power*, Vol. 17, No. 5, 2001, pp. 959–966.

[7]Rysanek, F., and Burton, R. L., "Effects of Geometry and Energy on a Coaxial Teflon Pulsed Plasma Thruster," AIAA Paper 2000-3429, July 2000.

[8]Markusic, T. E., Polzin, K. A., Levine, J. Z., McLeavey, C. A., and Choueiri, E. Y., "Ablative Z-Pinch Pulsed Plasma Thruster," AIAA Paper 2000-3257, July 2000.

[9]Dunning, J. W., Benson, S., and Oleson, S., "NASA's Electric Propulsion Program," International Electric Propulsion Conf., Paper IEPC-01-002, Oct. 2001.
[10]Zakrzwsky, C., Benson, S., Sanneman, P., and Hoskins, A., "On-Orbit Testing of the EO-1 Pulsed Plasma Thruster," AIAA Paper 2002-3973, July 2002.
[11]Bushman, S. S., "Investigations of a Coaxial Pulsed Plasma Thruster," M.S. Thesis, Univ. of Illinois, Urbana–Champaign, IL, May 1999.
[12]Muller, L., "Modelling of an Ablation Controlled Arc," *Journal of Physics D: Applied Physics*, Vol. 26, 1993, pp. 1253–1259.
[13]Domejean, E., Chevrier, P., Fievet, C., and Petit, P., "Arc-Wall Interaction Modelling in a Low-Voltage Circuit Breaker," *Journal of Physics D: Applied Physics*, Vol. 30, 1997, pp. 2132–2142.
[14]Kukhlevsky, S. V., Kaiser, J., Samek, O., Liska, M., and Erostyak, J., "Stark Spectroscopy Measurements of Electron Density of Ablative Discharges in Teflon-$(CF_2)_n$ Capillaries," *Journal of Physics D: Applied Physics*, Vol. 33, 2000, pp. 1090–1092.
[15]Hong, D., Dussart, R., Cachoncinlle, C., Rosenfeld, W., Gotze, S., Pons, J., Viladrosa, R., Fleurier, C., and Pouvesle, J. M., "Study of a Fast Ablative Capillary Discharge Dedicated to Soft X-Ray Production," *Review of Scientific Instruments*, Vol. 71, No. 1, 2000, pp. 15–19.
[16]Gatsonis, N. A., and Yin, X., "Axisymmetric DSMC/PIC Simulation of Quasi-neutral Partially Ionized Jets, AIAA Paper 97-2535, July 1997.
[17]Boyd, I. D., Keidar, M., and McKeon, W., "Modeling of a Pulsed Plasma Thruster from Plasma Generation to Plume Far Field," *Journal of Spacecraft and Rockets*, Vol. 37, No. 3, 2000, pp. 399–407.
[18]Keidar, M., Boyd, I. D., and Beilis, I. I., "Electrical Discharge in the Teflon Cavity of a Coaxial Pulsed Plasma Thruster, *IEEE Transactions on Plasma Science*, Vol. 28, No. 2, 2000, pp. 376–385.
[19]Keidar, M., Boyd I. D., and Beilis, I. I., "On the Model of Teflon Ablation in an Ablation-Controlled Discharge," *Journal of Physics D: Applied Physics*, Vol. 34, June 2001, pp. 1675–1677.
[20]Beilis, I. I., "Parameters of the Kinetic Layer of Arc Discharge Cathode Region," *IEEE Transactions on Plasma Science*, Vol. PS-13, No. 5, 1985, pp. 288–290.
[21]Wentink, T., "High Temperature Behavior of Teflon," AVCO-Everett Research Lab., Rept. AF 04 (647)-278, Everett, MA, July 1959.
[22]Keidar, M., Fan, J., Boyd, I. D., and Beilis, I. I., "Vaporization of Heated Materials into Discharge Plasmas," *Journal of Applied Physics*, Vol. 89, No. 6, 2001, pp. 3095–3098.
[23]Ruchti, C. B., and Niemeyer, L., "Ablation Controlled Arc," *IEEE Transactions on Plasma Science*, Vol. 14, No. 4, 1986, pp. 423–434.
[24]Kovatya, P., and Lowke, J. J., "Theoretical Predictions of Ablation-Stabilised Arcs Confined in Cylindrical Tubes," *Journal of Physics D: Applied Physics*, Vol. 17, 1984, pp. 1197–1212.
[25]Griem, H. R., *Plasma Spectroscopy*, McGraw–Hill, New York, 1964.
[26]Zemskov, A. I., Prut, V. V., and Khrabrov, V. A., "Pulsed Discharge in Dielectric Chamber," *Soviet Physics—Technical Physics*, Vol. 17, 1972, pp. 285–289.
[27]Andrianov, A. M., Zemskov, A. I., Prut, V. V., and Khrabrov, V. A., "Pulsed Discharges in Dielectric Chambers," *Soviet Physics—Technical Physics*, Vol. 14, No. 2, 1969, pp. 318–321.
[28]Kozlov, G. I., Kuznetsov, V. A., and Masyukov, V. A., "Radiative Losses by Argon Plasma and the Emissive Model of a Continuos Optical Discharge," *Soviet Physics—JETP*, Vol. 39, No. 3, 1974, pp. 463–468.
[29]Kovatya, P., "Thermodynamic and Transport Properties of Ablated Vapors of PTFE, Alumina, Perspex and PVC in the Temperature Range 5000-30000 K," *IEEE Transactions on Plasma Science*, Vol. 12, 1984, pp. 38–42.
[30]Schmahl, C. S., and Turchi, P. J., "Development of Equation-of-State and Transport Properties for Molecular Plasmas in Pulsed Plasma Thrusters. Part I: A Two-Temperature Equation of State for Teflon," *Proceedings of the International Electric Propulsion Conference*, 1997, pp. 781–788.
[31]Burton, R. L., Hilko, B. K., Witherspoon, F. D., and Jaafari, G., "Energy-Mass Coupling in High-Pressure Liquid-Injected Arcs," *IEEE Transactions on Plasma Science*, Vol. 19, No. 2, 1991, pp. 340–349.
[32]Spanjers, G. G., Lotspeich, J. S., McFall, K. A., and Spores, R. A., "Propellant Losses Because of Particulate Emission in a Pulsed Plasma Thruster," *Journal of Propulsion and Power*, Vol. 14, No. 4, 1998, pp. 554–559.
[33]Shapiro, A., *The Dynamics and Thermodynamics of Compressible Fluid Flow*, Wiley, New York, p. 102.
[34]Raizer, Y. P., *Gas Discharge Physics*, Moscow, Nauka, 1987 (in Russian), p. 229.
[35]Bekefi, G., *Radiation Processes in Plasmas*, Wiley, New York, p. 96.